Modeling the effect of striker geometry on the wave propagation pattern in the Split-Hopkinson pressure bar test using the discrete element method

Majid Nikkhah [a, *], Mahdi Bajolvand [a]

[a] *Faculty of Mining, Petroleum and Geophysics, Shahrood University of Technology, Shahrood, Iran.*

ABSTRACT

Split Hopkinson Pressure Bars (SHPB) test is widely used among the various methods for investigating the dynamic behavior of rocks at high strain rates. Various factors affect the waveform and the results of this test. In this study, the aim was to investigate the effect of geometrical parameters of strikers including the effect of shape, length, and impact cross-section width (ICSW) on the waveform induced in the SHPB test using numerical modeling. For this purpose, in the first stage, the required information including geometrical properties and the required micro-parameters have been collected from two laboratory and numerical modeling studies. Then, the initial model was constructed using the discrete element numerical method (DEM), and its results were compared with laboratory and numerical results. Evaluation of the effect of striker shape demonstrated that SS strikers have induced a semi-sinusoidal wave and CS strikers have induced a quasi-rectangular wave. Among the waveform properties, the wavelength was strongly related to the geometric properties of the strikers in both CS and SS types in a way that was directly related to the striker's length and inversely related to the ICSW. On the other hand, the maximum amplitude is directly related to the striker's length and ICSW in both CS and SS types. According to the results, the use of SS strikers is more appropriate according to the waveform, and its geometric properties can be determined according to the problem requirement, using numerical modeling results.

Keywords: *Split Hopkinson Bar Test (SHPB), Dynamic modeling, High strain rates, Waveform, Discrete element method.*

1. Introduction

Evaluating the behavior of materials and determining their properties are essential to the design of most engineering projects under different loads. Several in-situ and laboratory tests are performed for such purposes. Various methods are available to assess the dynamic behavior of concrete, rock, metal, and composites under a wide range of strain rates and various loading conditions. In this regard, some of the most important techniques are the Split Hopkinson Pressure Bar (SHPB) test, Taylor impact test, drop weight machines, and shock loading by plate impact. Moreover, high-speed imaging techniques and optical methods are used to analyze the behavior of materials under dynamic loading conditions [1]. Among the mentioned techniques, the SHPB test is most commonly applied in various loading modes (e.g., pressure, tensile, shear, and torsion) in order to assess the behavior of materials under high dynamic rate loading [2, 3].

The SHPB test is widely used as a laboratory test for the assessment of the strength properties of concrete, rocks, and metals under dynamic loading with high strain rates (HSRs). The test encompasses a striker and two bars (incident and transmitted) with the specimen placed between the aforesaid two bars. The test stages involve the induced stress wave as a result of the impact of a striker on the incident bar and reaching the specimen through the incident bar. The stress wave (incident wave) propagates along the incident bar towards the specimen. While part of the wave is transmitted to the specimen through the interface of the incident bar-specimen, another part of the wave is reflected from the interface. Following that, the wave transmitted to the specimen reaches the bar through the interface of the specimen-

transmitted bar. Finally, an energy absorber is often installed close to the end of the transmitted bar so as to damp the movement of the transmitted bar after testing. The stress, strain, and strain rate of the specimen could be calculated using Equation. 1 to Equation. 3, respectively [4].

$$\sigma = \frac{A_b}{2A_s} E_s \left[\varepsilon_I(t) + \varepsilon_R(t) + \varepsilon_T(t) \right] \tag{1}$$

$$\varepsilon = \frac{C_b}{L_s} \int_0^t \left[\varepsilon_I(t) - \varepsilon_R(t) - \varepsilon_T(t) \right] dt \tag{2}$$

$$\dot{\varepsilon} = \frac{C_b}{L_s} \left[\varepsilon_I(t) - \varepsilon_R(t) - \varepsilon_T(t) \right] \tag{3}$$

Where σ, ε, $\dot{\varepsilon}$, E, A, and L are stress, strain, strain rate, elastic modulus, cross-sectional area, and length, respectively, and C is the wave velocity. The subscripts I, R, and T represent the incident, reflected, and transmitted parts, respectively. Also, the subscripts b and s represent the bar and specimen, respectively.

The Split-Hopkinson pressure bar (SHPB) test is applied in rock engineering projects and discussions of rock dynamics to assess the dynamic behavior of rocks under dynamic loadings, such as explosion and projectile impact. Considering the excessively high loading rate of explosions, loading is applied to the samples under high loading rates in the SHPB test.

The traditional and conventional forms of the SHPB test use the Cylindrical shape Striker (CS) and bars. This approach has some limitations such as difficulty in achieving uniform stress and stress

* Corresponding author: *Tel:* +98 2332392204, *E-mail address:* m.nikkhah@shahroodut.ac.ir (M. Nikkhah).

equilibrium in the specimen and high oscillation of the generated wave [5, 6]. CS strikers generate a rectangular stress wave in the incident bar and specimen. On the other hand, this wave takes a very short time to reach the maximum strain compared to the time required to create a uniform stress state in the specimen. Therefore, the shape of the striker must change, so that it could have a semi-sinusoidal shape to reach the maximum level. In this regard, a model of the SHPB test has been proposed where a SS striker is applied to induce a semi-sinusoidal stress wave (Figure 1(a)). The geometry of the SS striker in the test is shown in Figure 1(b). The stress waveform induced by the striker with a special conical shape has a semi-sinusoidal waveform, leading to low-wave scattering during wave propagation [7]. In addition, it is possible to evaluate the dynamic behavior of rocks during the post-failure stage by this test [8]. The SHPB test is applied to conventional systems, while CS is used for the dynamic tests of metallic materials.
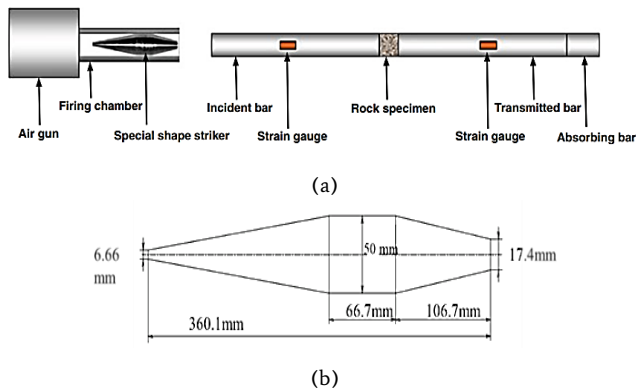

(a)

(b)

Figure 1. SHPB test; a) striker, incident, transmitted bars, and rock specimen; b) geometry of special-shape striker [9].

Figure 2 shows the classification of various dynamic tests, which are used to evaluate the dynamic behavior of rocks in different ranges of strain rates. According to [10], the classification indicates the rock conditions in these methods, including the creep behavior of rocks with the strain rate of 10^{-8} - 10^{-6} per second and quasi-static behavior with the strain rate of 10^{-5} - 10^{-1} per second, as well as moderate, high, and very high strain rate behaviors. Furthermore, numerical simulation provides efficient access for the implementation of testing and data analysis for the following reasons: 1) repetitive simulations with completely identical numerical samples could be performed, 2) the approximation could be obtained before experimental tests for guidance, and 3) details are available at any given time even in dynamic modes [11]. The high cost of manufacturing laboratory equipment is one of the reasons that has limited the sensitivity analysis studies of the geometrical properties of Striker-Bar assembly. Therefore, numerical modeling approaches can be used due to low time and cost with acceptable accuracy to model a wide range of geometry of Striker-Bar assembly and also choose the waveform appropriate to the purpose of the problem.

According to the literature, the SHPB test, which is applied to various materials, uses different forms of strikers, lengths of the bars, and specimen geometries. Diversity is observed in the geometry, length, and type of the striker and pressure bars [12, 13]. Moreover, samples of loaded materials (e.g., rocks, metal, and ceramics) have been studied in different dimensions and geometries [14]. Xu et al. [11] have demonstrated that numerical modeling could be applied based on the discrete element approach to simulate dynamic fracture and for the modeling of the SHPB test. In the mentioned study, acceptable results were obtained following the assessment of the dynamic behavior and fracture toughness of rocks using numerical modeling of the discrete element method. Peng et al. [9] evaluated rock dynamic features using the SHPB test in the laboratory. In addition, the researchers assessed the results using numerical methods in ANSYS/LS-DYNA. Liao et al. [15]

evaluated the behavior of rock specimens under compressive and shear loadings using the Hopkinson test, concluding that the numerical models could effectively simulate the behavior of rocks under such loading. In [12], it was experimentally demonstrated that the length of the striker could affect the wave pattern. Also, using the experimental and numerical finite element methods [13] and discrete element method [11] have demonstrated that the geometry of the striker affects the created waveform. Therefore, the geometric characteristics of the striker have been a challenge in the test to assess the dynamic behavior of materials.
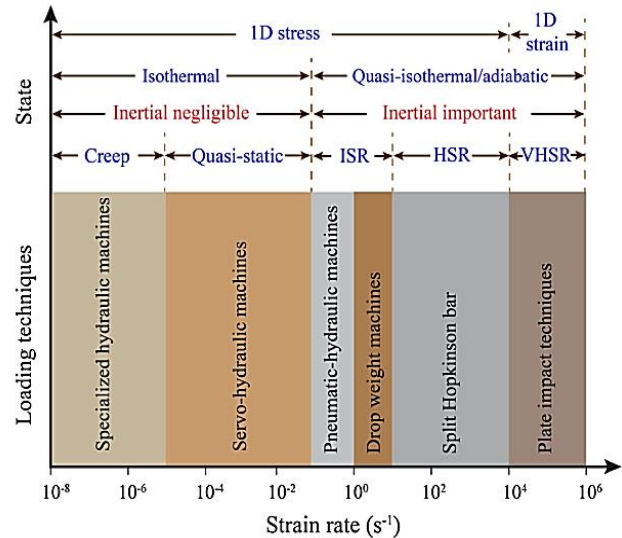

Figure 2. Classification of dynamic loading methods and rock conditions at various strain rates [10].

Accordingly, considering the capability of numerical modeling and the limitation of laboratory equipment in high strain/load rate condition simulations, in this study, DEM numerical modeling was performed to investigate the effect of geometrical parameters of striker including the effect of shape, length, and, impact cross-section width (ICSW) on the waveform induced in the SHPB test. The structure of this paper is as follows: In Section 2, the methodology (including data gathering, numerical modeling, and sensitivity analysis steps) is presented. In Section 3, the results of the study including verification of the initial model and other sensitivity analysis results are presented. In the end, in Section 4, the main results and recommendations are presented.

2. Material and Methods

In this study, the aim was to investigate the effect of geometrical parameters of striker including the effect of shape, length, and impact cross-section width (ICSW) on the induced wave in the SHPB test using numerical modeling. For this purpose, as shown in Fig.ure 3, in the first stage, required data have been collected from two laboratory and numerical modeling studies. Then, the initial model was constructed using the discrete element numerical method (DEM), and its results were compared with laboratory and numerical results. Then, the validated model has been used for the sensitivity analysis stage. In the sensitivity analysis, the characteristics of the induced waveform including maximum amplitude, wavelength, and wave velocity were evaluated from the impact of 10 models of cylindrical (CS) and specific shape (SS) striker types.

2.1. Data Gathering

In this research, laboratory and numerical studies performed by Zhao et al., 2011 [16] and Li et al., 2014 [4] have been used, the data of which are in Table. 1 and Table. 2. According to Zhao et al. and considering the

properties of Tabel.1, the results of SHPB test have shown that when the striker (specific_shape in Figure 1(b)) is shot toward the incident bar at the velocity of 10 m/s, a semi sinusoidal stress wave of 170 MPa is generated in the incident bar, which reaches one meter to the free section of the incident bar and strain gauge, approximately 360 milliseconds after the impact (Figure 4). Regarding the numerical modeling, Li et al [4] showed that the PFC2D software could carry out the process of the impact and transfer of the resulting stress wave with high accuracy and the lowest level of simplification. According to the high agreement of the results obtained from the modeling with the numerical model and experimental results of the aforementioned researchers, their findings were used for model validation in this research.

Figure 3. Flowchart of the current study.

Table 1. Test equipment properties [16].

Properties	Unit	Value
Incident bar length	mm	1500
Incident bar width	mm	50
Transmitted bar length	mm	750
Transmitted bar width	mm	50
Striker's length	mm	360.1
Striker's ICSW	mm	17.4
Striker and bars elastic modulus	GPa	240
Striker and bars density	(kg/m³)	7800
Striker impact velocity	(m/s)	10

2.2. Numerical Modeling of SHPB Test

A particle model of the striker, incident, and transmitted bars was developed in the PFC2D (Particle Flow Code2-Dimension) software to evaluate the wave-induced by various geometries of the striker considering the properties which are presented in Table 1 and Table 2.

PFC is based on the Distinct Element Method (DEM), which considers the material and structure to be analyzed as the composition of particles. PFC models the synthetic materials composed of an assembly of variably-sized rigid particles that interact at contacts to represent both granular and solid materials. The particles are treated as individual members to find force and displacement acting on the particle. PFC simulates the mechanical behavior of a system with included shaped particles [17, 18].

Table 2. Micro-parameters properties for numerical modelling of SHPB Test [4]

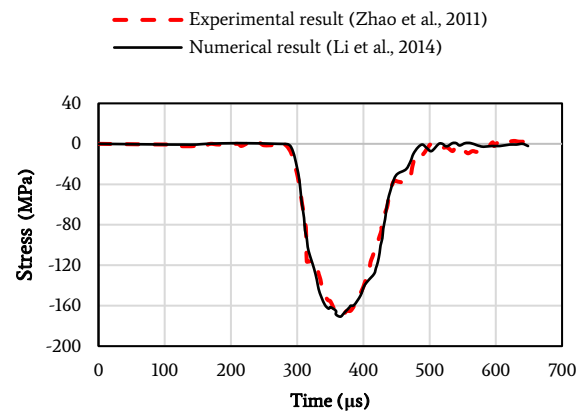| Element	Characteristics	Value
Discs	Minimum radius (mm)	0.9
	Maximum radius (mm)	1.5
	Normal stiffness(N/m)	6.86×10^{11}
	Shear stiffness(N/m)	2.45×10^{11}
	Density(kg/m³)	7894.7
	Porosity (%)	0
Bonds	Model Type	Contact bound
	Normal strength (MPa)	1×10^{100}
	Shear strength (MPa)	1×10^{100}
	Internal friction coefficient	0.577

Figure 4. Waveform induced in experimental and numerical results.

2.3. Sensitivity Analysis of Waveform

In this section, the sensitivity analysis of the effects of the striker's geometry has been done on the characteristics of the propagated waveform in the incident bar of the SHPB. Two scenarios of changes in the length and cross-sectional area at the interface between striker and incident bar were considered for each striker, which is further discussed in the following sections.

2.3.1. Effect of Striker's Shape

In order to analyze the effect of a striker's shape on a waveform, two types of strikers including Cylindrical (CS) (in 2D, it appears as a rectangular shape) and Specific-shape (SS) Strikers have been modeled as shown in Figure 5. These two types of strikers have the same length 360.1 mm and impact cross-section of 17.4 mm with different geometry.

2.3.2. Effect of Striker's Length

In order to analyze the effect of striker's length on the waveform, two types of striker shapes including cylindrical and specific shaped strikers with three lengths named CS I, CS II, CS III, SS I, SS II, and SS III have been modeled shown in Figure 6 and Figure 7. These six types of strikers have the same impact cross-section of 17.4 mm with different lengths of 360.1, 260.1, and 160.1 mm for CS and SS strikers, respectively.
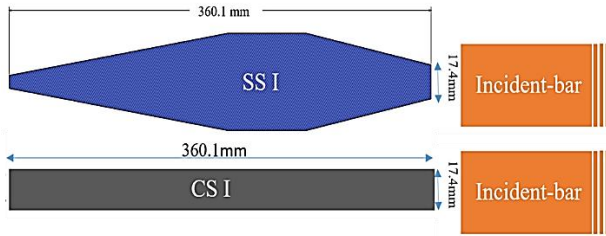
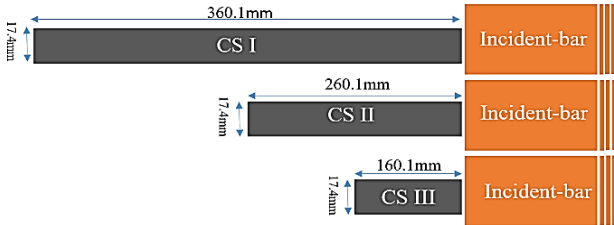**Figure 5.** Two types of strikers are used for shape effect analysis on the waveform.

Figure 6. The geometry of CS strikers with different lengths and the same cross-sections.
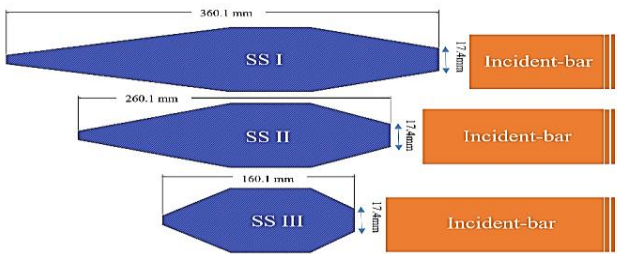

Figure 7. The geometry of SS strikers with different lengths and the same cross-sections.

2.3.3. Effect of Striker's ICSW

In order to analyze the effect of a striker's impact cross-section width on the waveform, two types of striker shapes including cylindrical and specific-shaped strikers with three impact cross-section widths named CS I_1, CS I_2, CS I_3, SS I_1, SS I_2, and SS I_3 have been modeled as shown in Figure 8 and Figure 9. These six types of strikers have the same length 360.1 mm with different impact cross-section widths 17.4, 33.7, and 50 mm for CS and SS strikers, respectively.

3. Results and Discussions

3.1. Numerical Modeling and Verification

The developed particle model of the SHPB test, including 27329 discs, is shown in Figure 10. As is observed, the particles had regular arrangement at the point of the interface of the incident-transmitted bars and striker-incident bar for the full transmission of the wave. In addition, the five measuring points of A, B, C, D, and E with a circle diameter of 15 mm were placed along the bar to measure stress at various times.

As mentioned earlier, numerical modeling validation was carried out by comparing the results of the numerical modeling in terms of stress versus time at a one-meter distance from the striker and impact velocity of 10 m/s in the incident bar with the results of the numerical and experimental studies of [16] and [4] as shown in Figure 11(a). Also, data, from highlighted regions in Figure 11(a), are presented in Table. 3 for more accurate comparisons. The accuracy value is calculated using Equation. 4 and Equation. 5, as follows:

$$Avg\ Error = \frac{\sum_{t=1}^{n}(A_t - AEX,\ ANU_t)}{n} \tag{4}$$

$$RMSE = \sqrt{\frac{\sum_{t=1}^{n}(A_t - AEX,\ ANU_t)^2}{n}} \tag{5}$$

Where t is time, A is amplitude resulting from this study, and AEX and ANU are amplitude from experimental results [16] and numerical modeling results [4]. As shown in Figure 11(b) and Figure 11(c), the accuracy of the initial model was 87% and 81% compared to the laboratory and numerical studies, respectively. Accordingly, this model can be used in the sensitivity analysis stage.

Figure 12 shows the wave pattern induced in the incident and transmitted bars during various steps of the SHPB. Figure 13 illustrates the waveform in the incident-pressure bars of the SHPB, caused by the impact of the SS striker at the velocity of 10 m/s in the model. In this respect, Stage I is the stage of the impact and formation of a semi-sinusoidal stress wave at the outset of the incident bar and striker interface. Stage II involves the traveling of the wave throughout the bar, passing from the measurement points A, B, C, and D. According to the findings, the stress wave was completely transmitted to the transmitted bar by reaching the end of the incident bar in Stage III. In Stage IV, the stress wave entering the transmitted bar travels through the bar, reaching the E measurement point at the mentioned time and moving to the end of the bar. By reaching the end of the bar in Stage V, the induced wave takes a tensional form and moves throughout the bar with a changed sign.
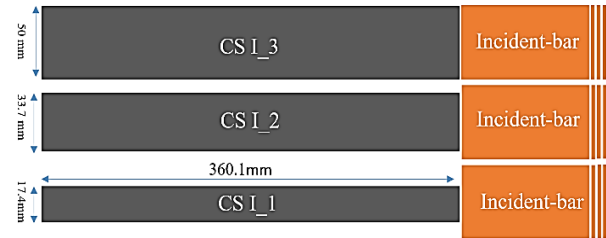

Figure 8. The geometry of CS strikers with different cross-sections and the same lengths.
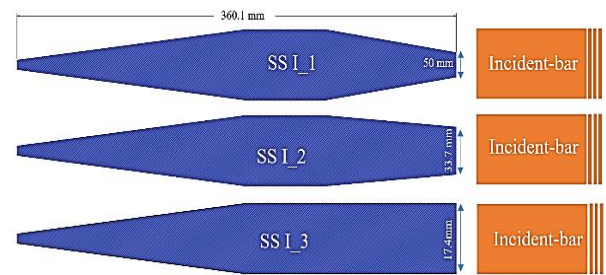

Figure 9. The geometry of SS strikers with different cross-sections and the same lengths.

3.2. Sensitivity Analysis of Waveform

3.2.1. Strikers Shape Effect

In Table. 4, the characteristics of the wave resulting from two models of strikers in two types CS and SS with unique 17.4 mm ICSW and 360.1mm lengths are presented. Also, Figure 14 shows the waveform resulting from the impact of the CS and SS strikers with the same ICSW and lengths. It can be seen that the waveform resulting from SS striker impact is semi-sinusoidal, which is similar to the results of the tests performed in [16] compared to an approximately rectangular waveform from CS striker impact. Also, the maximum amplitude resulting from SS striker impact has been obtained as approximately two times bigger than the maximum amplitude in CS striker type. On the other hand, wave travel time in SS striker impact is faster than in CS striker impact.
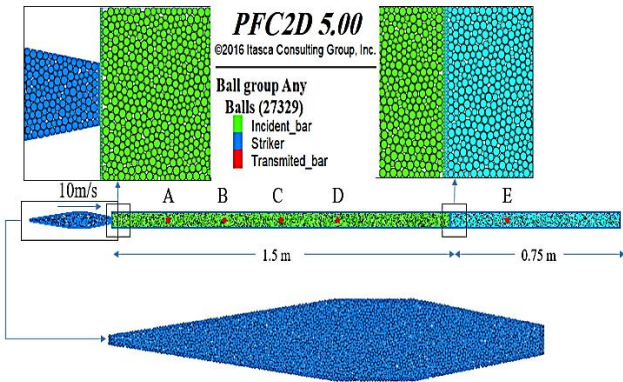
Figure 10. Particle model of striker, incident bar, transmitted bar, and measurement points of A, B, C, D, and E.
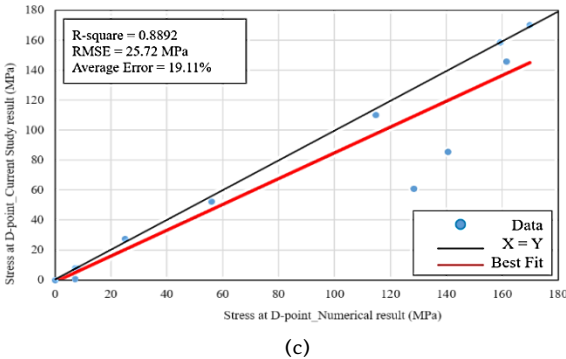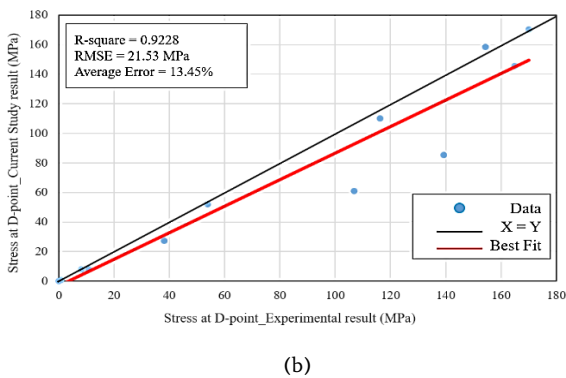
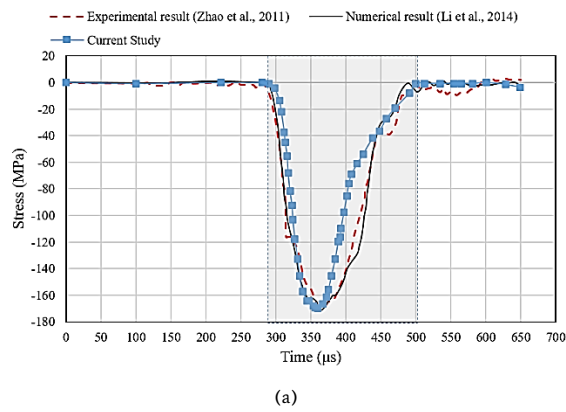**Table 3.** Comparison of compressional stress measured at D-point in the incident bar in representative times (in the range 280 – 500 μs).

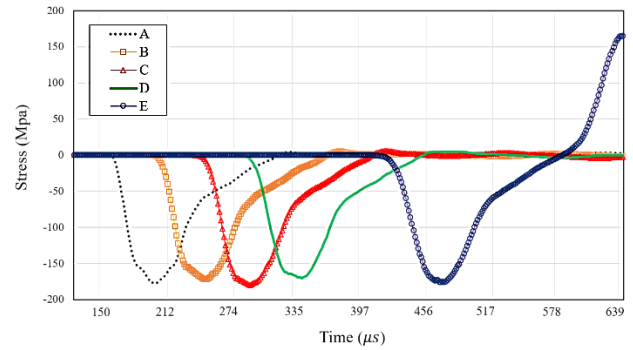| No.	Time (μs)	Current study	Experimental result (Zhao et al., 2011)	Numerical result (Li et al., 2014)
1	280	0.00	0.00	0.00
2	300	-7.85	-8.10	-8.01
3	320	-110.00	-116.27	-114.83
4	340	-158.50	-154.31	-159.33
5	360	-170.10	-170.10	-169.80
6	380	-145.69	-165.07	-161.48
7	400	-85.41	-139.23	-140.67
8	420	-61.00	-106.94	-128.47
9	440	-52.20	-53.83	-55.98
10	460	-27.27	-38.04	-25.12
11	480	-7.89	-10.77	-7.22
12	500	-0.72	-0.72	-7.18

(a)

Figure 12. Wave propagation pattern in bars of SHPB test by the impact of SS striker.

(b)

Figure 13. Different stages of induced stress wave and propagation by the impact of striker in bars.

(c)

Figure 11. Model results verification; a) comparison of waveform resulting from the current study with experimental and numerical modeling, b) accuracy of the model rather than experimental study, c) accuracy of the model rather than numerical modeling study.

Table 4. Characteristics of propagated wave in the incident bar from different shape strikers.

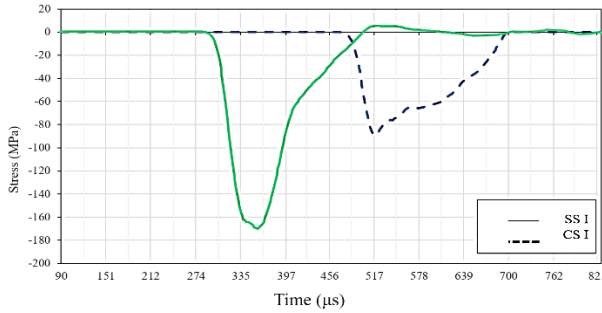| Properties	Unit	CS I	SS I
Striker's length	mm	360.1	360.1
Striker's ICSW	mm	17.4	17.4
Wave amplitude	MPa	89.34	170.41
Wave velocity[-1]	μs/m	519	359
Wavelength	μs	240	220

Figure 14. Waveform resulting from SS and CS impact.

3.2.2. Strikers Length Effect

In Table. 5, the characteristics of the wave resulting from six models of striker in two types CS and SS with unique ICSW and 360.1, 260.1, and 160.1 mm lengths are presented. As is observed, the wave amplitude decreased in the CS strikers with a reduced length. While the traveling time of the wave decreased more significantly in the CS II striker compared to the CS I striker, it was extremely higher in the CS III type. Figure 15 shows the waveform resulting from the impact of the CS strikers with different lengths. It can be seen that the wave had an approximately rectangular shape and an extremely low rise time. In addition, the wavelength decreased with the reduction of the striker length. The wave pattern formed by this striker had high oscillation, and another prominent feature was the non-uniformity of the induced wave compared to the semi-sinusoidal mode, which is a favorable shape for a test wave.

Table 5. The waveform characteristics resulting from length analysis of SS and CS Strikers.

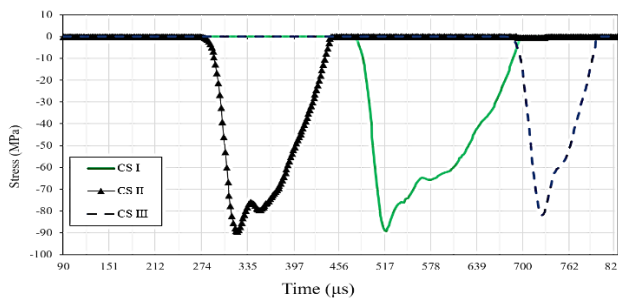| Properties	Unit	Striker types					
		CC I	CC II	CC II	SS I	SS II	SS III
Striker's length	mm	360.1	260.1	160.1	360.1	260.1	160.1
Striker's ICSW	mm	17.4	17.4	17.4	17.4	17.4	17.4
Max amplitude	MPa	89.34	89.27	81.92	170.41	173.76	173.21
Wave velocity[1]	μs/m	519	322	727	359	483	282
Wave length	μs	240	166	80	220	148	110

Figure 15. Waveform resulting from CS strikers impact with different lengths.

In SS strikers, the decreased length led to a different behavior for the CS type. Decreased striker length resulted in increased wave amplitude. Meanwhile, the traveling time of the wave decreased in the SS II type compared to the SS I type, whereas it extremely increased in the SS III type. Figure 16 depicts the stress waveform resulting from the numerical modeling of the effect of this striker. As is observed, the shape of the wave is semi-sinusoidal, which is similar to the results of the tests performed in [16]. Similar to the CS strikers, the wavelength decreased with reduced striker length. Moreover, the shape of the wave changed from smooth to non-smooth and sharp. This type of wave also has extremely low oscillation and maintains stability throughout the bar.

The sensitivity analysis plots of induced waveform versus different lengths of two types of strikers are shown in Figure 17. As demonstrated, among the waveform properties, the wavelength and maximum amplitude were directly related to the striker's length in both CS and SS types. However, the study of the wave velocity does not show a clear relationship with the striker's length. Also, the study of the oscillation on the induced waves shows that the waves resulting from the SS types are much less oscillating than the waves resulting from the CS types.
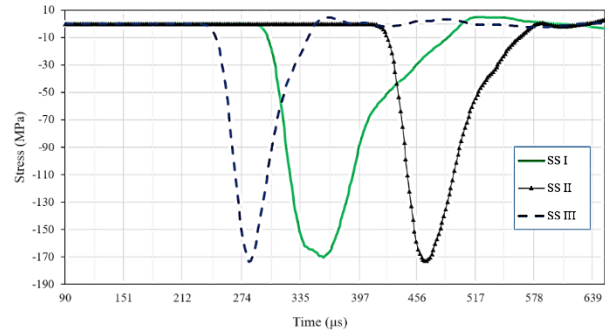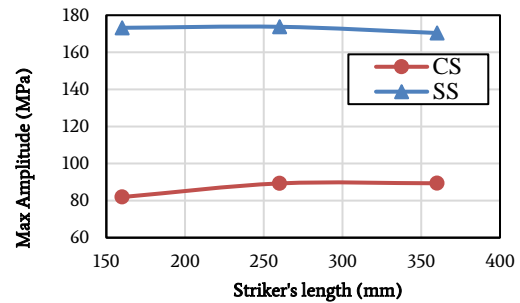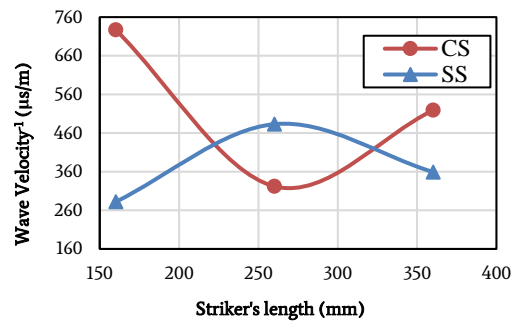

Figure 16. Waveform resulting from SS strikers impact with different lengths.
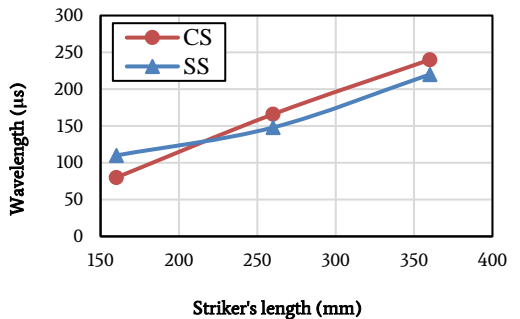

(a)

(b)

Figure 17. The sensitivity analysis plots of induced waveform versus different lengths for (a) Max amplitude, (b) wave velocity, and (c) wavelength.

3.2.3. Strikers ICSW Effect

In Table 6, the characteristics of the wave resulting from six models of strikers in two types CS and SS with unique lengths and 17.4, 33.7, and 50 mm ICSW are presented. Accordingly, in CS striker type, the wave amplitude significantly increased with the increased impact cross-section width. In addition, the traveling time of the wave decreased in the CS I-2 striker compared to the CS I-1 striker, whereas it extremely increased in the CS I-3 striker. Figure 18 shows the waveform resulting from the impact of the CS strikers with different ICSW. As illustrated in Figure 18, the induced wave has an almost approximately rectangular shape, and the wavelength is not significantly affected by the impact cross-section of the striker. Furthermore, this type of wave has high oscillation.

In SS strikers, the wave amplitude increased with the increased impact cross-section. On the other hand, the traveling time of the wave decreased in the SS I-2 striker compared to the SS I-1 striker, whereas it extremely increased in the SS I-3 striker. Figure 19 depicts the shape of the stress wave resulting from the modeling process. As is shown in Figure 19, the induced waves have a semi-sinusoidal form, and similar to the CS strikers shows that the wavelength is not affected by the impact cross-section of the striker. In addition, the waveform remained stable with the least oscillation along the bar.

The sensitivity analysis plots of induced waveform versus different ICSW of two types of strikers are shown in Figure 20. As demonstrated in Figure 20, among the waveform properties, the wavelength was inversely related to the ICSW in both CS and SS types. On the other hand, the maximum amplitude is directly related to the striker's ICSW in both CS and SS types. However, the study of the wave velocity does not show a clear relationship with the striker's ICSW.

Table 6. The waveform characteristics resulting from ICSW analysis of SS and CS strikers

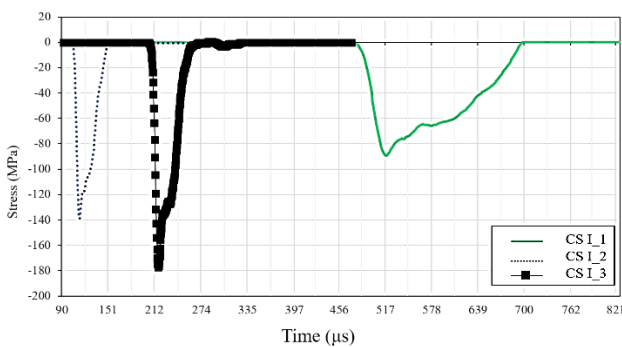| Properties	Unit	Striker types					
		CC I	CC I-2	CC I-3	SS I	SS I-2	SS I-3
Striker's length	mm	360.1	360.1	360.1	360.1	360.1	360.1
Striker's ICSW	mm	17.4	33.7	50	17.4	33.7	50
Max amplitude	MPa	89.34	137.14	177.61	170.41	171.87	177.54
Wave velocity[-1]	µs/m	519	123	220	359	550	196
Wave length	µs	240	51	74	220	65	54

Figure 18. The shape of propagated stress wave in the incident bar from the impact of CS striker with different cross-sections

Figure 19. The shape of propagated stress wave in the incident bar from the impact of SS striker with different cross-sections.

(a)

(b)

(c)

Figure. 20. The sensitivity analysis plots of induced waveform versus striker's ICSW for (a) Max amplitude, (b) wave velocity, and (c) wavelength.

4. Conclusion

In the present research, the discrete element method (DEM) was used to evaluate the effects of the striker's geometry on the characteristics of the waves induced in the incident bar of the SHPB test. The numerical modeling of the two CS and SS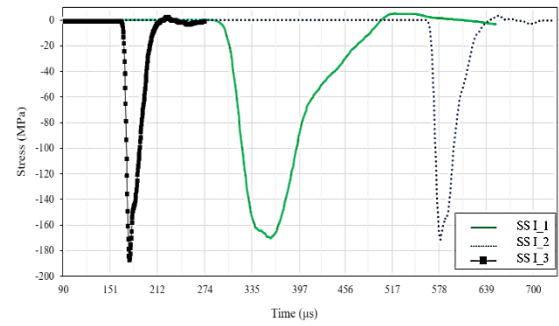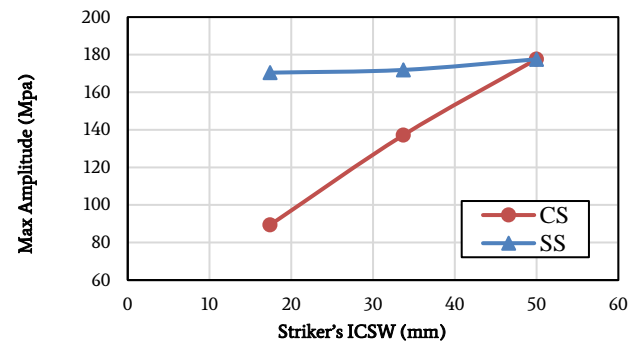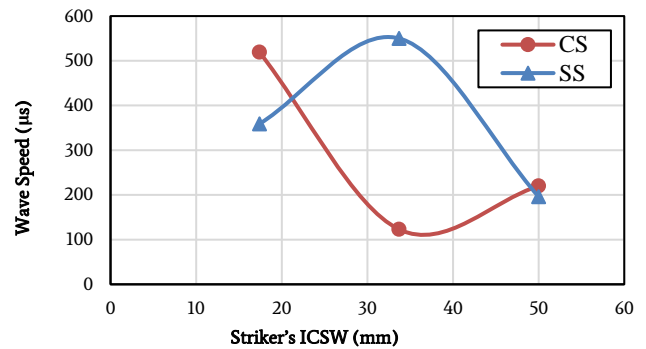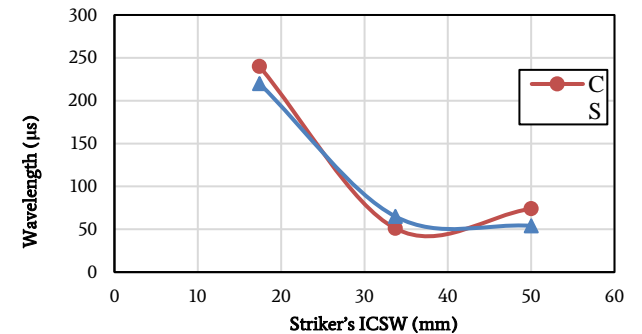 strikers was performed, and the characteristics of the waves resulting from the impact of each striker were assessed by changing the length and cross-section of the striker. Some of the most important results of the study are as follows:

- The discrete element method could properly simulate the

propagation of the waves induced and propagated by impact in the split Hopkinson pressure bar dynamic test. Such ability provides an opportunity to model specific geometries for each experimental assessment within a short time and in a cost-efficient manner using the software for the evaluation of the resulting wave and its propagation in the bar.

- A direct correlation was observed between the striker length and wavelength of the induced wave which was observed in both the CS and SS strikers.
- The waves resulting from the impact of the CS strikers have an approximately rectangular shape, while the wave-induced from the SS strikers with trimmed-cone have the semi-sinusoidal and semi-triangular compressive waveform in both modes of length and ICSW change.
- Among the waveform properties, the wavelength was strongly related to the geometric properties of the strikers in both CS and SS types in a way that was directly related to the striker's length and inversely related to the ICSW.
- The maximum amplitude is directly related to the striker's length and ICSW in both CS and SS types.
- The study of the wave velocity does not show a clear relationship between the striker's length and ICSW.
- The study of the oscillation on the induced waves shows that the waves resulting from the SS types are much less oscillating than the waves resulting from the CS types.
- Therefore, according to the results, the use of SS strikers is more appropriate according to the waveform rather than CS Strikers. Also, the SS striker's geometric properties can be determined according to the problem requirement, using numerical modeling results.

Because of some limitations such as laboratory data, this research focused on the striker's geometrical properties and effects on the induced waveform. It can be useful if some researchers focus on impact velocity effect, rock, and other critical materials behavior under induced load from this test, etc. using the proposed workflow in this study.

REFERENCES

[1] Aziznejad S, Esmaieli K, Hadjigeorgiou J, Labrie, D (2018) Response of jointed rock masses subjected to impact loading. J Rock Mech and Geotech Eng 10(4), 624-634, https://doi.org/ 10.1016/j.jrmge.2017.12.006.

[2] Majzoobi G.H, Rahmani K, Lahmi S (2019) Determination of length to diameter ratio of the bars in torsional Split Hopkinson bar. Measurement 143, 144 154, https://doi.org/10.1016/ j.measurement.2019.04.054.

[3] Gerlach R, Kettenbeil C, Petrinic N (2012)A new split Hopkinson tensile bar design. Int J Impact Eng 50, 63-67, https://doi.org /10.1016/j.ijimpeng.2012.08.004.

[4] Li, X, Yang Z, Zhou Z (2014) Numerical Simulation of the Rock SHPB Test with a Special Shape Striker Based on the Discrete Element Method. Rock Mech Rock Eng 47:1693–1709, https://doi.org/10.1007/s00603-013-0484-6.

[5] Lok T.S, Li X.B, Liu D.S, Zhao P.J (2002) Testing and response of large diameter brittle materials subjected to high strain rate. J Material Civil Eng 14(3):262–269, https://doi.org/10.1061/ (ASCE)0899-1561(2002)14:3(262).

[6] Li X.B, Lok T.S, Zhao J, Zhao P.J (2000) Oscillation elimination in the Hopkinson bar apparatus and resultant complete dynamic stress–strain curves for rocks. Int J Rock Mech Min Sci 37(7):1055–1060, https://doi.org/10.1016/S1365-1609(00)00037-X.

[7] Kolsky H (1949) An investigation of the mechanical properties of materials at very high rates of loading. Proc Phys Soc Lond SerB 62(11), 676–700, https://doi.org/10.1088/0370-1301/62/11/302.

[8] Zhou Z.l, Li X, Liu A, Zou Y (2017) Dynamic behavior of rock during its post failure stage in SHPB tests. Transactions of Nonferrous Metals Society of China 27(1), 184-196, https://doi.org/10.1016/S1003-6326(17)60021-9.

[9] Peng K, Gao K, Liu J, Liu Y, Zhang Zh, Fan X, Yin X, Zhng Y, Huang G (2017) Experimental and Numerical Evaluation of Rock Dynamic Test with Split-Hopkinson Pressure Bar. Advances in Materials Science and Engineering, Article ID 2048591, https://doi.org/10.1155/2017/2048591.

[10] Zhang Q.B, ZhaoJ (2014) A Review of Dynamic Experimental Techniques and Mechanical Behaviour of Rock Materials. Rock Mech Rock Eng 47:1411–1478, https://doi.org/ 10.1007/s00603-013-0463-y.

[11] Xu Y, Dai F, Xu N.W, Zhao T (2016) Numerical Investigation of Dynamic Rock Fracture Toughness Determination Using a Semi-Circular Bend Specimen in Split Hopkinson Pressure Bar Testing. Rock Mech Rock Eng 49:731–745, https://doi.org/ 10.1007/s00603-015-0787-x.

[12] Chen X, Ge L, Zhou J, Wu S (2015) Experimental Study on Split Hopkinson Pressure Bar Pulse-Shaping Techniques for Concrete. J Material and Civil En 28(5): 04015196, 1-9. https://doi.org/10.1061/(ASCE)MT.1943-5533.0001494.

[13] Baranowski P, Malachowski J, Gieleta R, Damaziak K, Mazurhiewicz L, Kolodziejcyk D (2013) Numerical study for determination of pulse shaping design variables in SHPB apparatus. Technical science 61)2(, 459-466, https://doi.org/ 10.2478/bpasts-2013-0045.

[14] Panowicz R, Janiszewski J, Kochanowski K (2019) Effects of Sample Geometry Imperfections on the Results of Split Hopkinson Pressure Bar Experiments. Experimental Techniques 43:397–403, https://doi.org/10.1007/s40799-018-0293-7.

[15] Liao Z.Y, Zhu J.B, Xia K.W, Tang C.A (2017) Determination of Dynamic Compressive and Tensile Behavior of Rocks from Numerical Tests of Split Hopkinson Pressure and Tension Bar. Rock Mech Rock Eng 49(10), 3917-3934, https://doi.org/10.1007/ s00603-016-0954-8.

[16] Zhou ZL, Li X.B, Liu A.H, Zou Y (2011) Stress uniformity of split Hopkinson pressure bar under half-sine wave loads. Int J Rock Mech Min Sci 48(4):697–701, https://doi.org/10.1016/ j.ijrmms.2010.09.006.

[17] Itasca Consulting Group Inc (2016) PFC2d user's manual, version 5.0. Minneapolis

[18] Nikkhah M (2017) Numerical assessment of influence of confining stress on Kaiser effect using distinct element method. Journal of mining and environment 8(2): 215-226 https://doi.org/10.22044/jme.2016.674